ceed a minimum strength for stability $k_0 < k$. This result agrees with rigid body results insofar as it is stable for large k.

Viscous damping in the rod-plate coupling can be treated in simple fashion. To include viscous damping in our equations, we replace k by $cs + k$ where c is the damping coefficient. The root locus expression can be written as $-1/k = G(s)$. With damping included this becomes $-1/cs + k) = G(s)$. If we let $k/c = m$, we can write $-1/c = (s + m)G(s)$. We can now treat m as a parameter and sketch the root loci for this expression. We shall give a representative sketch for case 1 treated previously for rotation about the minimum axis (see Fig. 4). The sketch in Fig. 4 assumes that $m > 0$; however, the general nature of the root locus remains the same as m is varied. It can be seen from Fig. 4 that the system is unstable for all c, and our previous discussion indicates that this is true for all m as well. Thus, this system is unstable for all values of c ($c \neq 0$) and all values of k. By similar investigations, the other cases except case 4 are found to be unstable regardless of the sign of the damping constant. Damping is destabilizing in case 4 for negative damping but stabilizing if $c > 0$. That damping is destabilizing for all but major axis rotation is to be expected, but that negative damping is not stabilizing about the minimum axis is contrary to what one might expect from energy considerations. We can treat viscous damping in all coordinates for small damping constants by noting the displacement of the poles and zeroes. With this technique, we can show that small damping forces of appropriate signs and relative magnitudes can make the system asymptotically stable.

The results we have obtained are based on an analysis of the linearized equations of motion of the physical system. Asymptotic stability of the linearized system is sufficient for asymptotic stability of the motion, but simple stability is not sufficient for stability of motion. It is necessary, however, and the fact that the linear motion is stable means that, though the system may not be stable, the drift away from equilibrium takes place relatively slowly so that stability could be achieved by implementing a control system which employs small control forces. As an example, suppose that by reason of external constraints it became necessary to maintain rotation about the intermediate axis. Clearly, the system employing the semielastic scheme could be controlled by a much smaller and hence lighter system.

To demonstrate our results, we devised a simple free-fall experiment, using a model constructed from cardboard and scotch tape, and the use of paper clips as counterweights to provide the desired moments of inertia. The scotch tape not only held the two moving parts together but provided the elasticity. By addition of bracing supports we were able to make the coupling variable from elastic to rigid without requiring a change in the distribution of mass. We arranged the masses so that the moments of inertia were configured as in case 2 (intermediate axis rotation). At first the coupling was made rigid. As expected, when the model was tossed spinning into the air, it began to tumble wildly after less than a second of flight. This was repeated several times with similar results each time. This result was not surprising since we know a rigid body is unstable about its intermediate axis. Next we relaxed the coupling so that it was no longer rigid. This time when the model was tossed spinning into the air, there was no tumbling, and the model continued to spin smoothly throughout its flight, dramatically demonstrating the effect.

We have shown that motion about the intermediate axis can be made stable for a body structured like a dually rotating space station might be and that it could be advantageous to make the coupling between spun and despun parts elastic in order to enhance the controllability of such a vehicle. This investigation was conducted in order to explore some of the problems of rotating space stations in Earth orbit and their possible solutions. The author is not aware of any other work along this line having been done.

Experimental Results on Crosshatched Ablation Patterns

HANS W. STOCK* AND JEAN J. GINOUX†
von Kármán Institute for Fluid Dynamics, Rhode-Saint-Genèse, Belgium

DURING recent years surface patterns created during ablation on re-entry or wind-tunnel models have been the subject of considerable interest. They appeared in form of streamwise striations, turbulent wedges and criss-crossed grooves. Among these, the latter has been studied the most intensively. Experimental results on patterns parameters are given in Ref. 1, 2, and 3. Although attempts have been made trying to explain the triggering mechanism[2–6] of the phenomenon, the problem is not yet solved.

In this Note, the results of an experimental program on crosshatching are presented.

1. Test Facility

Tests were made at a freestream Mach number of 5.3 with the following tunnel stagnation conditions

$$T_{ST} = 150\text{–}400°\text{C}$$

$$P_{ST} = 12\text{–}32\ \text{kgf/cm}^2$$

giving unit freestream Reynolds numbers of

$$1.3\text{–}3.8 \times 10^7/\text{m}$$

2. Models

The 10 to 50° total vertex angle cones and the 10° cones with 12 to 40° total flares were tested at zero angle of attack. Typical test results are shown in Fig. 1. The models had pointed steel noses and a maximum basic diameter of 8 cm.

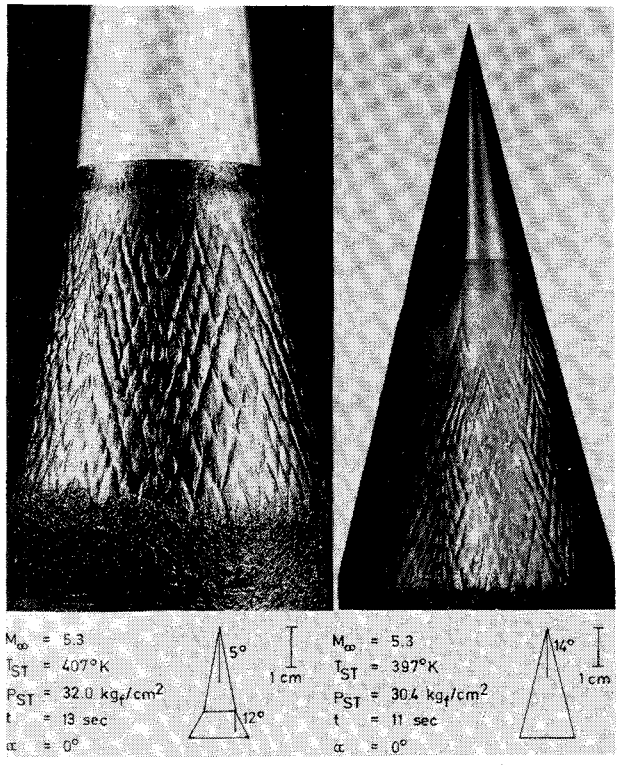

Fig. 1 Typical test results on wax models.

Received October 16, 1970.

* Research Assistant.
† Professor, Brussels University and Head of VKI Department of Supersonics and Hypersonics.

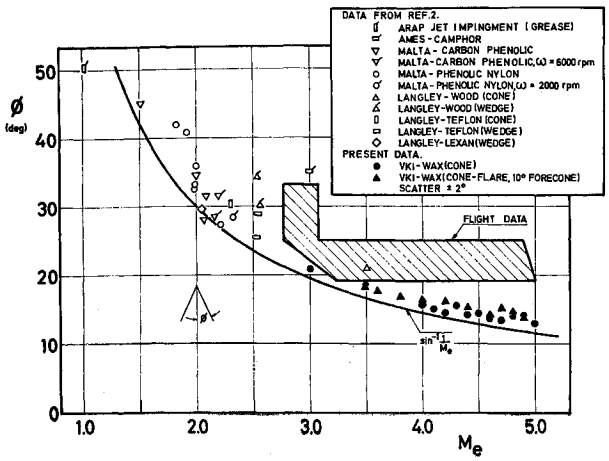

Fig. 2 Influence of the local Mach number M_e on the cant angle ϕ.

Local Mach numbers at the outer edge of the boundary layer of M_e = 3–5 and local static pressures of p_e = 0.05 to 0.35 kgf/cm² were provided. M_e and p_e were calculated by the tangent cone method ignoring viscous interaction and surface deformation caused by ablation.

3. Ablation Materials

Two ablation materials were tested, natural wax without seedings, which liquified under test conditions without vaporizing and camphor, a purely subliming material. Camphor models were obtained by sintering the powdered material in a vacuum under high pressure (500 kgf/cm²) using the technique of Charwat.[7]

4. Test Results

The effect of local Mach numbers M_e, local static pressure p_e and driving temperature ratio $(T_r - T_w)/T_w$ on the cant angle ϕ and the streamwise spacing λ of the criss-crossed grooves were measured from photographs taken after the runs.

4.1 Cant Angle ϕ

The cant angle ϕ is shown versus the local Mach number M_e in Fig. 2 and compared with the Mach angle (solid curve). Available wind tunnel and free flight data from Ref. 2 are shown for comparison. As seen, the present results follow the Mach angle trend in the Mach number range 3–5, contrary to the flight data for which "freezing" was observed above a Mach number of 3. It is possible that the difference comes from the fact that nose blunting occurred in free flight,

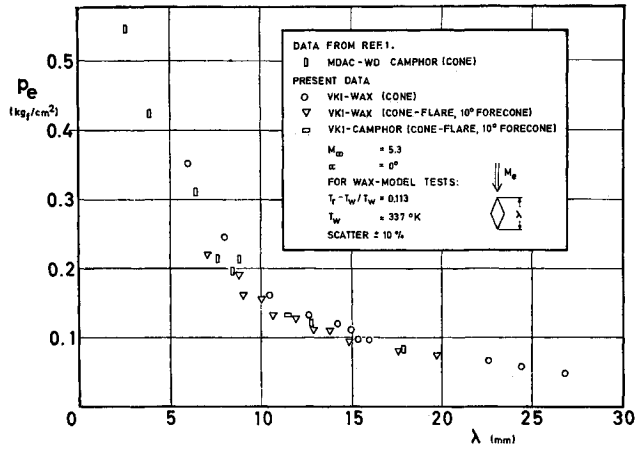

Fig. 3 Influence of the local static pressure p_e on the streamwise spacing λ.

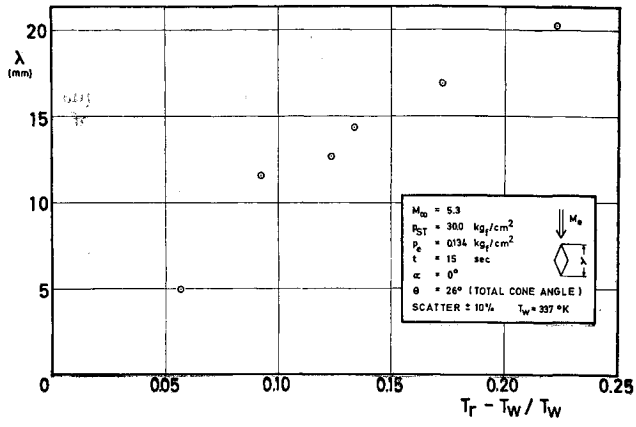

Fig. 4 Influence of the driving temperature ratio $(T_r - T_w)/T_w$ on the streamwise spacing λ.

while the present tests were made with models having pointed noses.

4.2 Streamwise Spacing λ

The effect of local surface pressure p_e on the streamwise spacing λ is shown in Fig. 3 for a fixed temperature ratio $(T_r - T_w)/T_w$ = 0.113. The results agree very well with those of Williams,[1] extending the range to lower static pressures and greater values of the streamwise spacing. T_r was computed by assuming a turbulent recovery factor of 0.895. T_w = 337°K is the temperature at which wax liquifies, independent of p_e. The surface pressure p_e was varied both by changing the cone or flare angle and thereby the local Mach number, and by altering the tunnel stagnation pressure. The local Mach number did not appear to have any influence on the spacing λ, when the static pressure and the driving temperature ratio were held constant.

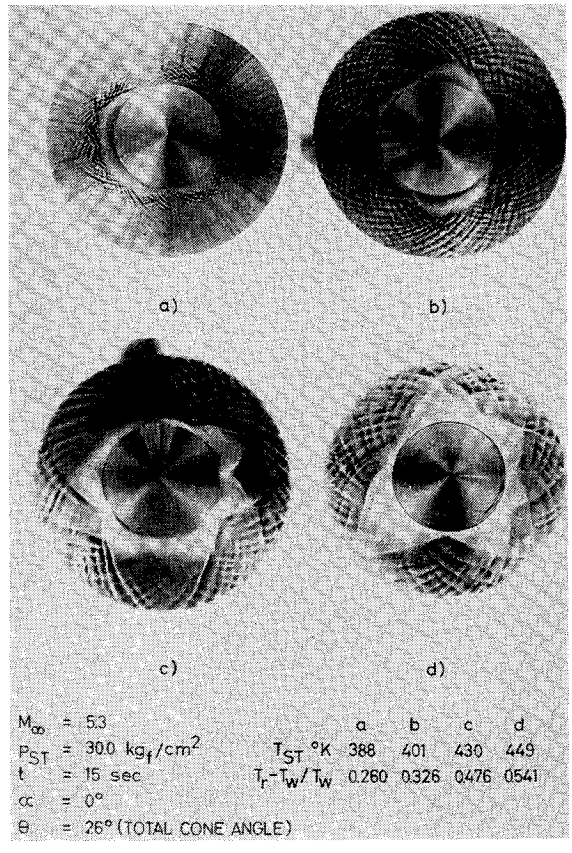

Fig. 5 Photographs of ablation patterns on cones showing the effect of driving temperature on λ.

The effect of driving temperature ratio $(T_r - T_w)/T_w$ on streamwise spacing λ measured on wax cones is shown in Figs. 4 and 5 for constant values of M_e and p_e. The streamwise spacing increases nearly linearly with the temperature ratio. A similar observation is presented in Fig. 1 of Ref. 3, where plexiglas which is also a liquifying ablation material was used. Reference 3 shows clearly that the pattern wavelength was nearly doubled when the stagnation temperature was increased from $T_{ST} = 750°K$ to 1070°K. It may be possible that the driving temperature dependence of the pattern size is characteristic of liquifying ablation materials. Camphor test results are not yet available.

4.3 Pattern Motion

For a few tests with wax models (both axisymmetric and two-dimensional) a movie was taken during the complete testing period. It showed a slow "creeping" motion of the whole crosshatched pattern in the streamwise direction of the order of 1 wavelength/10 sec.

References

[1] Williams, E. P., "Experimental Studies of Ablation Surface Patterns and Resulting Roll Torques," AIAA Paper 69-180, New York, 1969.

[2] Laganelli, A. L. and Nestler, D. E., "Surface Ablation Patterns: A phenomenology Study," AIAA Paper 68-671, Los Angeles, 1968.

[3] Canning, T. N. et al., "Orderly Three-dimensional Processes in Turbulent Boundary Layers on Ablating Bodies," AGARD Supplement to Conference Proceedings No. 30, May 1968,

[4] Mirels, H., "Origin of Striations on Ablative Materials," *AIAA Journal*, Vol. 7, No. 9, Sept. 1969, pp. 1813-1814.

[5] Tobak, M., "Hypothesis for the Origin of Cross-Hatching," *AIAA Journal*, Vol. 8, No. 2, Feb. 1970, pp. 330-334.

[6] Probstein, P. F. and Gold, H., "Cross-Hatching: A Material Response Phenomena," *AIAA Journal*, Vol. 8, No. 2, Feb. 1970, pp. 364-366.

[7] Charwat, A. F., "Exploratory Studies on the Sublimation of Slender Camphor and Naphtalene Models in a Supersonic Wind Tunnel," RM-5506-ARPA, July 1968, Rand Corporation.

Computation of Chebycheff Optimal Control

GERALD J. MICHAEL*
United Aircraft Research Laboratories, East Hartford, Conn.

I. Introduction

THE majority of optimal control problems appearing in the literature consist essentially of a system defined by the vector differential equation

$$\dot{x} = f(x,u,t), \quad x(t_0) = x_0, \quad u\epsilon U \tag{1}$$

and a Bolza-type optimality criterion

$$J[u] = \int_{t_0}^{t_f} h(x,u,t)dt + F[x(t_f),t_f]$$

where x represents the vector state of the system, U denotes a set of admissable controllers, and t_0,t_f denote initial and final times, respectively. Optimal control u^* is defined as that control in U which minimizes the performance criterion J, i.e., u^* is defined by $J[u^*] = \min_u J[u]$. Well-known analytic and computational techniques exist for the solution of such Bolza-type optimization problems. On the other hand, there are many situations when the performance criterion J is not conveniently representable as a line integral. Such situations occur when it is desired to minimize the maximum or peak value of some pertinent time function as, for instance, power or percent overshoot. In these cases the performance criterion is given by $J[u] = \max_t g[x(t)]$ and optimal control u^* is defined by $J[u^*] = \min_u \max_t g[x(t)]$ for $u\epsilon U$ and $t\epsilon[t_0,t_f]$. Performance criteria of this type are not generally amenable to a Bolza formulation and are, in fact, termed Chebycheff performance criteria after the Russian mathematician Chebycheff whose basic investigations in the 19th century led to the formulation and the solution of a broad class of min-max problems. For the Chebycheff optimal control problem, however, very few results are available.

Neustadt[1] considered a Chebycheff-type problem in which it is desired to transfer a linear system from one given state to another while minimizing the control effort, where effort is defined as the maximum control amplitude. Johnson[2] provided valuable insight into the Chebycheff problem by deriving certain geometric properties of a Chebycheff optimal controller, but his technique for explicitly determining optimal control is not amenable to digital computation and except for relatively simple systems, is prohibitively difficult to implement.

In this paper a general method is demonstrated for the efficient computation of Chebycheff optimal control for nonlinear systems. The algorithm is used to determine a Chebycheff optimal controller for the minimum flight path angle climb to station of an airbreathing vehicle whose thrust and fuel flow rate are characterized by a thrust coefficient and a specific impulse both of which are given as tabular functions of Mach number. Advantages of the proposed algorithm are pointed out as well as potential pitfalls which may be encountered in its implementation. The purpose of this paper is to demonstrate, by its application to a relatively sophisticated nonlinear system typical of those which occur in many practical aerospace flight control problems, that the proposed algorithm is a computationally feasible means of solving Chebycheff optimal control problems as well as to point out certain of its limitations.

II. Chebycheff Algorithm

The dynamic system is represented by Eq. (1) with t_0 specified, a final time $t_f \geq t_0$ implicitly defined by $\Omega[x(t_f)] = 0$, and $x_0\epsilon X$ where X is interpreted as the set of all states controllable by some $u\epsilon U$ to the manifold defined by $\Omega(x) = 0$. It is assumed that X is nonempty. The variational problem considered here is the minimization of

$$J[u] = \max_t g[x(t)] \tag{2}$$

with respect to $u\epsilon U$ for $t\epsilon[t_0,t_f]$ and subject to the differential constraint (1). In order to develop a computational procedure for approximating the Chebycheff optimal controller u^*, a theorem[3] is invoked which states that if $h(t)$ is nonnegative, single-valued, bounded, and continuous function on $[t_0,t_f]$ then

$$\max_t h(t) = \lim_{q\to\infty} \left\{\int_{t_0}^{t_f} [h(t)]^q dt\right\}^{1/q}$$

Then if g satisfies the previous conditions the Chebycheff criterion (2) can be replaced by the infinite sequence of performance criteria

$$J_q[u] = \left\{\int_{t_0}^{t_f} [g(x(t))]^q dt\right\}^{1/q}, \quad q = 1,2,\ldots$$

Since minimization of J is equivalent to minimization of the

Received November 9, 1970; revision received January 25, 1971. The author gratefully acknowledges valuable discussions with and the programming assistance of G. J. Thrasher of the Turbo Power and Marine Division of United Aircraft Corporation.

* Research Engineer, Simulation Laboratory.